

Defects evolution in n-type 4H-SiC induced by electron irradiation and annealing

Huifan Xiong^{1,2}, Xuesong Lu^{1,2}, Xu Gao^{1,2}, Yuchao Yan^{1,2}, Shuai Liu², Lihui Song^{1,2,†}, Deren Yang^{1,2}, and Xiaodong Pi^{1,2,†}

¹State Key Laboratory of Silicon and Advanced Semiconductor Materials & School of Materials Science and Engineering, Zhejiang University, Hangzhou 310027, China

²Key Laboratory of Power Semiconductor Materials and Devices of Zhejiang Province & Institute of Advanced Semiconductors, ZJU-Hangzhou Global Scientific and Technological Innovation Center, Zhejiang University, Hangzhou 311200, China

Abstract: Radiation damage produced in 4H-SiC by electrons of different doses is presented by using multiple characterization techniques. Raman spectra results indicate that SiC crystal structures are essentially impervious to 10 MeV electron irradiation with doses up to 3000 kGy. However, irradiation indeed leads to the generation of various defects, which are evaluated through photoluminescence (PL) and deep level transient spectroscopy (DLTS). The PL spectra feature a prominent broad band centered at 500 nm, accompanied by several smaller peaks ranging from 660 to 808 nm. The intensity of each PL peak demonstrates a linear correlation with the irradiation dose, indicating a proportional increase in defect concentration during irradiation. The DLTS spectra reveal several thermally unstable and stable defects that exhibit similarities at low irradiation doses. Notably, after irradiating at the higher dose of 1000 kGy, a new stable defect labeled as R_2 ($E_c - 0.51$ eV) appeared after annealing at 800 K. Furthermore, the impact of irradiation-induced defects on SiC junction barrier Schottky diodes is discussed. It is observed that high-dose electron irradiation converts SiC n-epilayers to semi-insulating layers. However, subjecting the samples to a temperature of only 800 K results in a significant reduction in resistance due to the annealing out of unstable defects.

Key words: 4H-SiC; deep level transient spectroscopy (DLTS); photoluminescence (PL); defects

Citation: H F Xiong, X S Lu, X Gao, Y C Yan, S Liu, L H Song, D R Yang, and X D Pi, Defects evolution in n-type 4H-SiC induced by electron irradiation and annealing[J]. *J. Semicond.*, 2024, 45(7), 072502. <https://doi.org/10.1088/1674-4926/23090024>

1. Introduction

In contrast to other wide bandgap semiconductors like diamond, silicon carbide (SiC) boasts the advantage of being available in larger dimensions, making it a popular choice as a substrate material for high-frequency and high-power devices^[1, 2]. Due to SiC's exceptional physical properties and impressive resistance to radiation, it is particularly attractive for applications in demanding fields such as aerospace^[3–5]. Research has demonstrated that SiC exhibits superior radiation resistance compared to conventional silicon materials, attributed to its higher atomic displacement energy^[4, 6]. However, it is crucial to note that SiC can still undergo degradation when subjected to high-energy particles, with the degree of damage depending on the irradiation dose. Numerous studies have examined the effects of various types of radiation, including electrons, protons, and neutrons, on SiC materials and device^[7–9]. High-speed electrons, which are the most common among radiation particles, have received considerable attention in recent research. These studies have explored the impact of electron irradiation on the performance of various SiC devices^[8, 10] and identify an increasing number of defects induced by irradiation in SiC through the use of various characterization tools, including deep level transient spectroscopy (DLTS) and photoluminescence (PL).

Existing literature reports electron irradiation can induce point defects in SiC, which include simple vacancies, interstitials, and some complex configurations. These defects can exhibit various energy levels and are classified as either donors or acceptors, each with a specific energy level. For example, typical vacancy defects contain the $Z_{1/2}$ and EH_7 defects. They are associated with the charge transition levels of carbon vacancies (V_C), specifically (0/2-) and (+/-) charge states^[11]. Furthermore, $Z_{1/2}$ is acknowledged as a double acceptor negative-U center in 4H-SiC, significantly contributing to the reduction of carrier lifetime^[12–14]. Silicon vacancy (V_{Si}) is another important type of point defect induced by electron irradiation in SiC. V_{Si} exhibits unique spin properties, facilitating its applications in scalable quantum information systems^[15–17]. Other point defects induced by electron irradiation, such as double vacancies ($V_{Si}V_C$)^[18–20] and carbon anti-site–carbon vacancy pairs ($C_{Si}V_C$)^[21, 22], possess comparable spin properties as V_{Si} in SiC. In addition, V_{Si} can be annealed out at temperatures ranging from 350 to 600 °C with an activation energy of 1.8 eV^[23, 24]. At elevated temperatures, V_{Si} will transform to $C_{Si}V_C$, necessitating an activation energy of approximately 2.5 eV^[25, 26]. Furthermore, $C_{Si}V_C$ serves as a strong carrier compensation center in n-type and semi-insulating SiC but will decompose into V_C and C_{Si} above 1200 °C^[21, 27].

In our research, we utilized 10 MeV high-energy electron irradiation on SiC Schottky barrier diodes (SBDs), ensuring uniform irradiation along the incident direction due to its substantial projected range (22 mm) in SiC. We carefully selected a broad range of irradiation doses, spanning from 50 to

Correspondence to: L H Song, songlihui@zju.edu.cn; X D Pi, xdpi@zju.edu.cn

Received 14 SEPTEMBER 2023; Revised 24 FEBRUARY 2024.

©2024 Chinese Institute of Electronics

3000 kGy, which allowed us to effectively monitor the evolution of defects as the irradiation doses increased. To identify the defects induced by electron irradiation, we employed both photoluminescence and deep level transient spectroscopy techniques. Additionally, we investigated the thermal stability of these induced defects and their impact on the electrical characteristics of SiC SBDs. Our study also explores the compensation effect resulting from induced electrically active defects, which can significantly impact SiC materials and devices.

2. Experimental

The starting material used in this study was a 13- μm thick n-type 4H-SiC epilayer with carrier concentration of approximately $5 \times 10^{15} \text{ cm}^{-3}$, grown on a SiC substrate doped with $1 \times 10^{18} \text{ cm}^{-3}$. The epilayer was sectioned into several $1 \times 1 \text{ cm}^2$ squares. Surface contamination was eliminated through Radio Corporation of America (RCA) cleaning before sputtering 200 nm nickel onto the C-face of the epilayer using magnetron-sputtering at the Nano Fabrication Center in Zhejiang University. Subsequently, the sample underwent annealing at 1050 °C for 2 min to form an Ohmic contact. Nickel Schottky contacts were fabricated on the opposite side through electron beam evaporation with a mask, followed by annealing at 500 °C for 5 min to minimize interface states. The Schottky contact electrodes, each with a diameter of 1 mm, were uniformly arranged on the square samples. Both annealing processes were conducted under flowing nitrogen gas in a rapid thermal processing furnace (RTP). The Schottky barrier diodes (SBDs) were subjected to electron irradiation at doses of 50, 500, 1000, 1500, 2000, 2500, and 3000 kGy, using a high energy 10 MeV electron accelerator with a pulse repetition frequency of 230 Hz at the Institute of Nuclear-Agricultural Science in Zhejiang University. The experimental setup for electron irradiation is depicted in Fig. 1. Casio simulations indicated that the SBD samples remained transparent during 10 MeV electron irradiation, with an adequate projected range of 22 mm on SiC. As a result, it can be inferred that defects were uniformly introduced throughout the entire thickness of the 360- μm samples.

Raman and PL measurements were conducted on the 4H-SiC epilayer at room temperature using a Horiba LabRAM Odyssey Raman microscope. Raman measurements were conducted with a laser at 532 nm and a 50x objective. The Raman spectra were collected over a range of 200–1800 cm^{-1} . For PL measurements, a laser at 266 nm and a 40x objective were employed. DLTS measurements were carried out using the DLS-80D system from SEMILAB in lock-in capacitance mode. DLTS spectra were recorded over a temperature range of 100 to 800 K, a range within which no alloying occurs between the electrode metal and silicon carbide, thereby eliminating any potential impact on the experimental results. DLTS measurement involves an annealing process executed in a vacuum sample chamber, with a heating rate of 0.2 K/s. Upon reaching the intended temperature, it is maintained for 4 min. It is worth noting that all subsequent annealing of the irradiated samples will be carried out using this method. The parameters used for DLTS measurements included a filling pulse value of $V_p = 0 \text{ V}$, a pulse width of $t_p = 42 \mu\text{s}$, and a reverse bias of $V_r = -5 \text{ V}$.

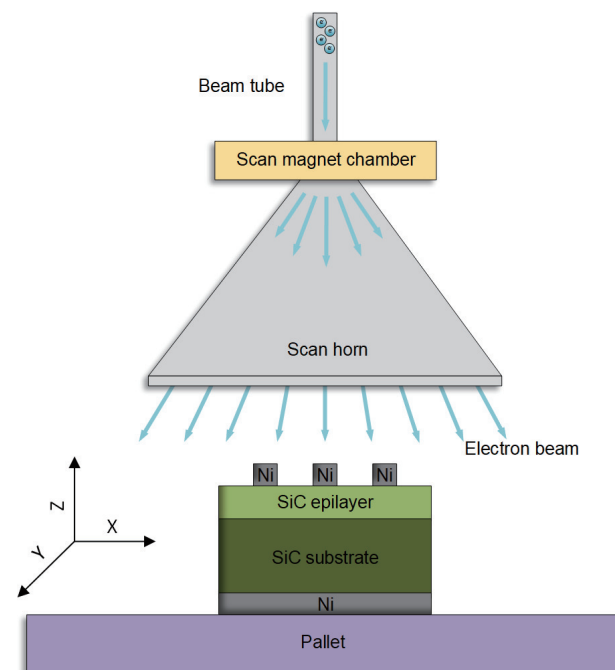


Fig. 1. (Color online) Experimental setup of electron irradiation. Schematic diagram illustrating the electron irradiation process for a 4H-SiC Schottky barrier diode (SBD).

3. Results and discussion

Both current–voltage (I – V) and capacitance–voltage (C – V) measurements were conducted on the irradiated samples before and after annealing at 800 K. Fig. 2(a) presents the I – V curves of the samples after irradiating at different doses, illustrating an increase in specific on-resistance with escalating doses. The ideality factor, calculated from the slope of the linear region of forward I – V characteristic, increases from 1.04 to 3.02 after irradiating at 500 kGy. It is important to emphasize that these parameter fittings are only applicable to samples irradiated at low doses, whose Schottky characteristics have not been significantly impacted. Meanwhile, the on-resistance is the most effective parameter in SBD samples irradiated at high doses. The elevation in on-resistance may be associated with free electrons captured by acceptor defects and the deionization of nitrogen impurities due to the displacement damage. It is evident from subsequent DLTS measurements that the defects induced by irradiation are predominantly acceptor defects, leading to a certain degree of depletion of free electrons. The greater the radiation dose that SiC is exposed to, the more defects are introduced. This leads to a larger compensation effect, thereby increasing the on-resistance. At a dose of 2500 kGy, the resistance of the SiC samples has reached a semi-insulating level^[28, 29]. However, the heating process at 800 K exerts a considerable impact on the resistance, causing a substantial reduction to several orders of magnitude smaller, as illustrated in Fig. 2(b).

Moreover, we conducted C – V measurements of the SBDs at a frequency of 1 MHz, with the bias range sweeping from –20 to 0 V. As the irradiation dose increased, the observed capacitance of the samples showed a corresponding decrease. As illustrated in Fig. 2(c), an irradiation dose of 1000 kGy induced a significant reduction in the capacitance

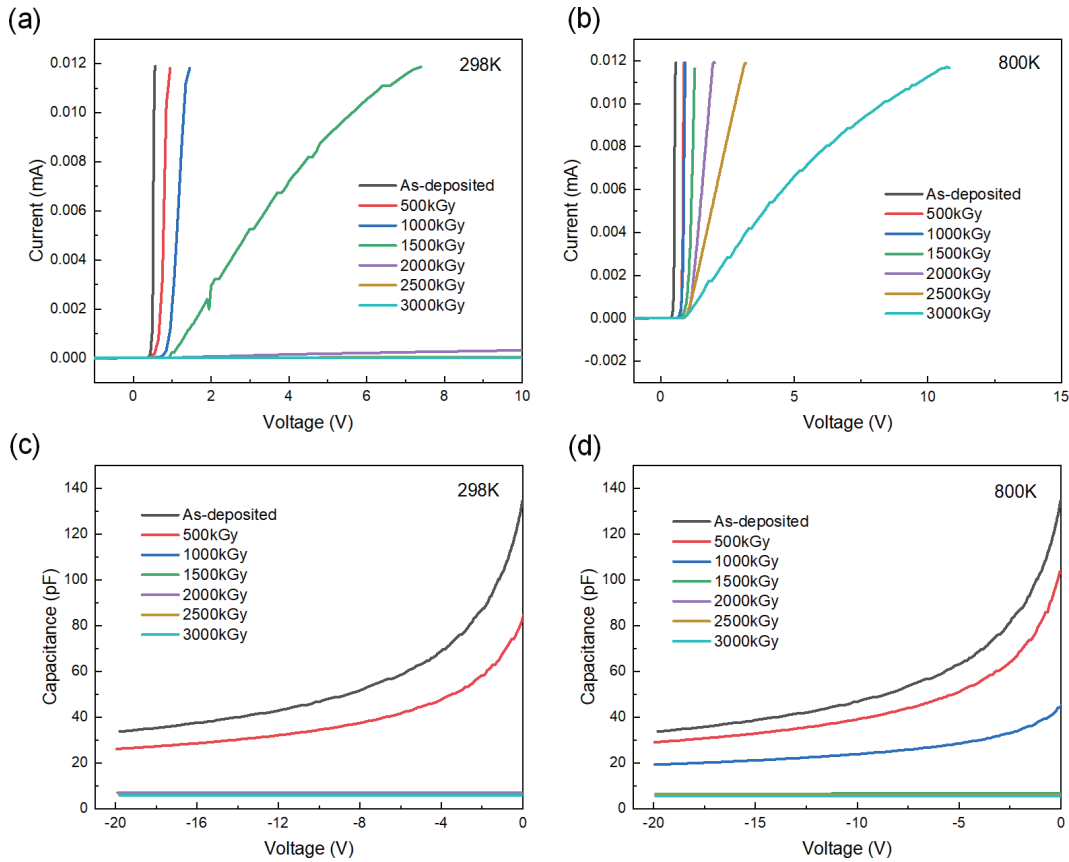


Fig. 2. (Color online) Electrical characterization. I - V curves of the 4H-SiC SBD irradiated with different doses before (a) and after (b) annealing at 800 K. C - V curves of the 4H-SiC SBD samples irradiated with different doses before (c) and after (d) annealing at 800 K.

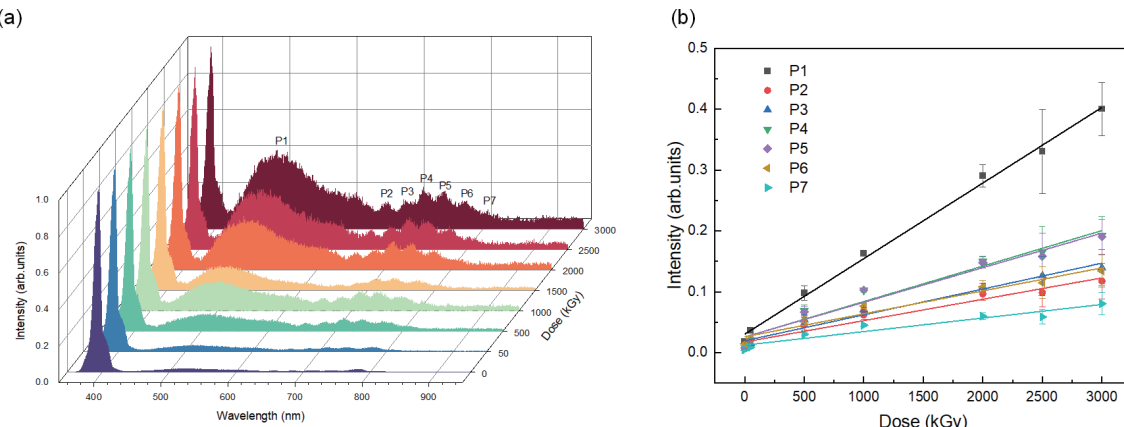


Fig. 3. (Color online) PL spectroscopy analysis. (a) PL spectra of SiC samples irradiated with different doses. (b) The linear relationship between irradiation dose and PL intensity of the peaks presented in (a).

to a minimal value, exhibiting negligible dependency on the bias voltage. This reduction in capacitance can be attributed to the augmentation in the quantity of electrically active defects induced by electron irradiation. The carrier concentration obtained from the $1/C^2$ versus V plots exhibited a significant decrease after irradiating at a dose of 500 kGy. These defects result in a reduction of the net carrier concentration and an expansion of the electric field within the depletion region, ultimately culminating in a decrease in capacitance. Furthermore, the influence of annealing on the capacitance is predominantly insignificant at high doses, as indicated in Fig. 2(d). In summary, electron irradiation exerts a considerable effect on the electrical characteristics of SiC SBDs, resulting in a degradation in rectification.

In order to evaluate the effects of electron irradiation on the crystal structures of SiC, Raman spectroscopy was employed prior to the identification of radiation-induced defects. Interestingly, the Raman spectra remained unaffected even under the influence of electron irradiation up to a dose of 3000 kGy. Subsequently, PL measurements were conducted at room temperature using a 266 nm laser. For quantitative analysis, all peak intensities were normalized based on the nitrogen-related peak (390 nm) in the near band edge region^[30]. Seven irradiation-induced peaks are detected in the PL spectra (Fig. 3(a)), with a prominent center at 500 nm. Additional peaks located at 66, 685, 713, 740, 775, and 808 nm were observed in the red and near-infrared bands, which are near the emission wavelengths of

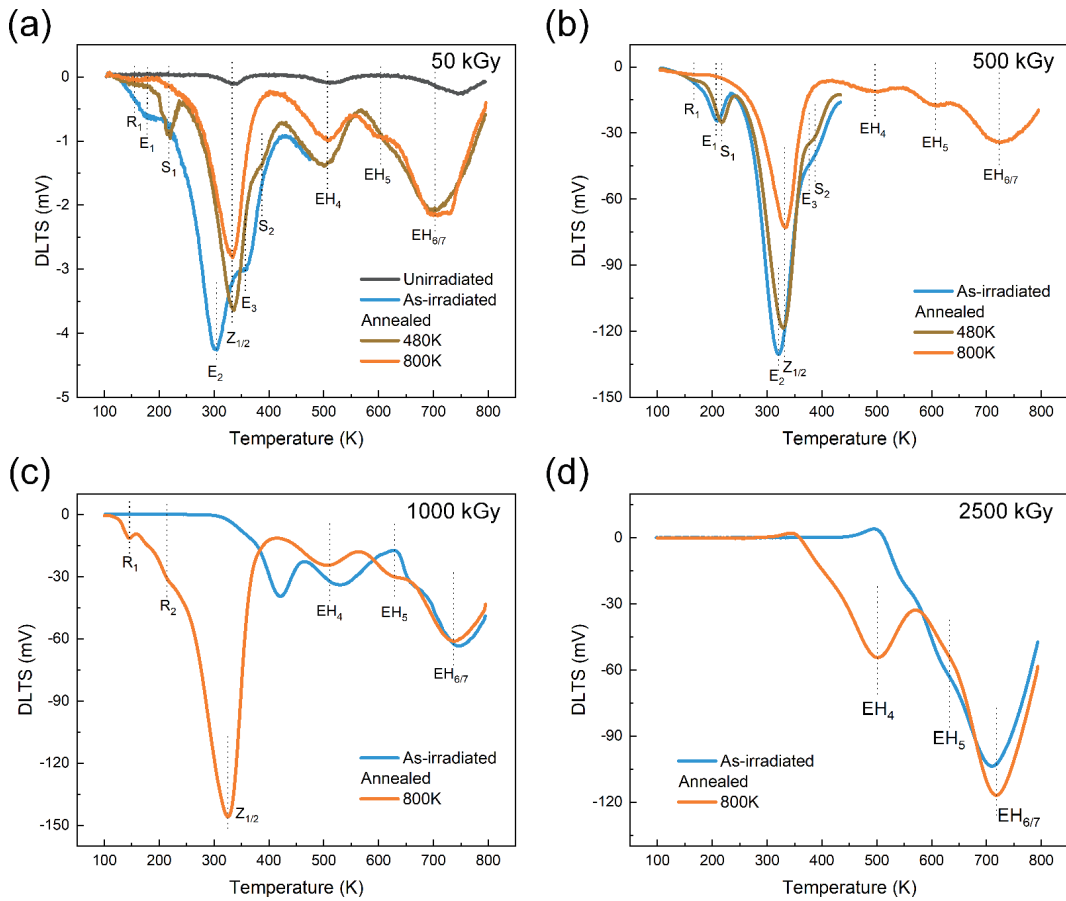


Fig. 4. (Color online) DLTS analysis. DLTS spectra of the n-type 4H-SiC irradiated with doses of 50 kGy (a) and 500 kGy (b) and after annealing at temperatures of 480 and 800 K. DLTS spectra measured at the irradiation dose of 1000 kGy (c) and 2500 kGy (d) before and after annealing at 800 K.

Table 1. Deep levels detected in 4H-SiC after electron irradiation and subsequent annealing.

Defects	$E_C - E_T$ (eV)	σ_n (cm^2)
R ₁ ^[37, 38]	0.24	6×10^{-16}
E ₁ ^[9, 38, 39]	0.35	3×10^{-16}
S ₁ ^[38–41]	0.40	3×10^{-15}
R ₂	0.51	6×10^{-14}
E ₂ ^[9, 38, 39]	0.58	3×10^{-16}
Z _{1/2} ^[38–41]	0.64	5×10^{-15}
E ₃ ^[9, 38, 39]	0.70	3×10^{-16}
S ₂ ^[38–41]	0.75	4×10^{-15}
EH ₄ ^[38, 39, 41, 42]	0.91	3×10^{-16}
EH ₅ ^[38, 39, 41, 42]	1.15	4×10^{-16}
EH _{6/7} ^[38, 39, 41, 42]	1.54	8×10^{-15}

$\text{Cs}_\text{Si}\text{V}_\text{C}$ ^[31–34]. Notably, the 500 nm peak typically appears in irradiated SiC and is attributed to donor–acceptor pairs involving a nitrogen atom and a structural defect^[35, 36]. Given its considerable concentration, this structural defect is presumed to be carbon vacancy. Moreover, a comparative analysis was performed on samples irradiated with varying doses, revealing a linear correlation between the irradiation doses and the concentration of these radiation-induced defects, as illustrated in Fig. 3(b).

We embarked on an investigation of the defects induced by irradiation, both pre and post-annealing, utilizing the deep level transient spectroscopy (DLTS) technique. Table 1 presents a comprehensive summary of the detected defects,

along with their identification parameters such as the energy level ($E_C - E_T$), the electron capture cross section (σ_n), and their potential identities. It is noteworthy that several thermally unstable defects can either disappear or transform into another defect when anneal between 300 to 700 K^[37, 38]. For instance, S₁ and S₂ defects can stably exist at 480 K and completely disappear at 800 K. Subsequently, we conducted DLTS measurements on SiC SBDs both before and after annealing at 480 and 800 K to reveal all the defects. Upon annealing at 480 K, we observed transformations from E₁, E₂, and E₃ to S₁, Z_{1/2}, and S₂, respectively, as illustrated in Fig. 4(a). This phenomenon has been reported in multiple studies involving both electron and ion irradiation^[38–41, 43], but no conclusive explanation exists. The variations in the DLTS peak positions contribute to the differences in emission rates, which are contingent on the difference between the defect energy level and conduction band edge. One explanation for this phenomenon is that the stress induced by defect clusters formed after irradiation alters the energy levels of surrounding defects. The subsequent heat treatment supplies the requisite energy to alleviate the stress, resulting in a shift in the energy levels of these defects. Another explanation is based on the changes in the conduction band edge of SiC material. It has been hypothesized that the 4H polytype could transform into 3C polytype (with smaller bandgap) after irradiation due to the formation of stacking faults. It is also worth noting that annealing-induced changes in the 3C region are conceivable within the 100–200 °C range, as suggested by density functional theory calculation^[44]. However, considering

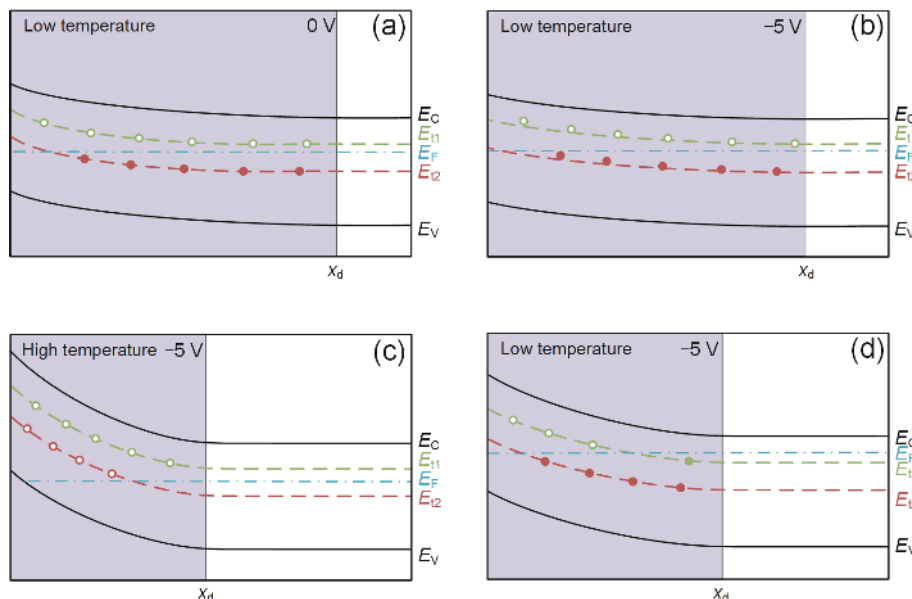


Fig. 5. (Color online) Influence of electric field and temperature on energy band diagram of the SBD device. Band structure of high-dose irradiated 4H-SiC at room temperature under the bias of 0 V (a), -5 V (b), and under high temperature with bias of -5 V (c). Band structure of 800 K-annealed 4H-SiC at room temperature under bias of -5 V (d). Note that the x axis is the depth direction from the surface and the x_d is the depletion region width.

the evidence from the Raman spectra and observation of this phenomenon post low-dose irradiation, our inclination is towards the first explanation provided above.

Fig. 4(b) presents the defects induced by electron irradiation at a dose of 500 kGy. It is noteworthy that the positions of E-centers (E_1 , E_2 , E_3) in the 500 kGy spectrum have shifted to the right compared to those in the 50 kGy spectrum. This shift is attributed to the increased thermal energy generated by electron irradiation at higher doses. It can be observed that the type of defects induced by irradiation is consistent at both 50 and 500 kGy. The S_1 and S_2 defects, previously identified as V_{Si} , were effectively eliminated upon annealing at 800 K. However, the $Z_{1/2}$ defect remains dominant both before and after annealing due to its robust thermal stability, playing a decisive role in the carrier compensation effect. The EH_4 and EH_5 defects exhibit close energy level positions and have been associated with distinct configurations of carbon antisite–carbon vacancy pair ($C_{Si}V_C$) at a single donor (+/0) level^[24]. However, their identification has been questioned. EH_4 is exclusively observed in samples irradiated with high-energy electrons, while EH_5 can be generated through 200 keV electron irradiation, which is known to introduce only carbon-related defects^[27]. Furthermore, $C_{Si}V_C$ is considered to be an isomer of the silicon vacancy, which can be transformed from a silicon vacancy when an adjacent carbon atom migrates to and subsequently occupies an empty silicon lattice site^[45, 46].

However, the defects in the low-temperature part of the DLTS spectra disappear when the dose reaches 1000 kGy, as illustrated in Fig. 4(c). It is essential to highlight that defects themselves do not disappear, but their signal in DLTS spectra disappears. The disappearance of defects presented in the low-temperature range of DLTS spectra could be attributed to the compensation effect caused by deep-level defects. Electron irradiation induces a significant quantity of defects, principally carbon vacancies ($Z_{1/2}$). These acceptor defects deplete the majority of free electrons, which originate from the ioniza-

tion of the nitrogen impurities. In this case, the Fermi energy level of SiC shifts below these defects presented in the low-temperature part of DLTS spectra, thus preventing them from capturing electrons under the applied pulse voltage. Consequently, the transient capacitance remains unaltered under reverse voltage, leading to no signal output. After annealing at 800 K, the previously undetected defects reappear in the DLTS spectra due to a reduction in the compensation effect as some defects are annealed out. We observed a defect labeled as R_1 ($E_C - 0.24$ eV), which is also observed in SiC after irradiating at lower doses, both before and after annealing. Although previously reported, its identification is still being discussed^[37, 38]. Additionally, we identified a new stable defect labeled as R_2 ($E_C - 0.51$ eV), as shown in Fig. 4(c). The R_2 defect could correspond to a complex (C_2)_{Si} defect with an energy level of $E_C - 0.50$ eV^[47]. As the irradiation dose increases, defect generation becomes more complex. When beyond 1000 kGy, more deep-level defects are produced, leading to a strengthened compensation effect, as shown in Fig. 4(d). In this case, carbon vacancy is rarely ionized and thus seldom deplete electrons due to the position of Fermi energy level being below the level of $Z_{1/2}$. The deeper-level defects are dominantly responsible to compensate the most of electrons ionized by nitrogen dopants. Consequently, only the deeper-level defects in the higher temperature range of the DLTS spectra can be detected. For instance, only one peak is observed in the DLTS spectrum of the samples irradiated at a dose of 2500 kGy. The DLTS technique thus provides a visual representation of the compensation effect in semiconductor materials.

The compensation effect arising from irradiation dose and annealing effects can be elucidated using the energy band diagram depicted in Fig. 5. The energy levels of the lower-level defect E_{t1} and the deeper-level defect E_{t2} are represented by the dashed green and red lines, respectively. The depletion region is shaded in purple. Under high irradiation doses, the induced defects function as acceptors and is able

to capture electrons, resulting in a significant compensation effect. Consequently, this leads to a shift in Fermi energy level towards the middle of the bandgap. Meanwhile, the capacitance of the SBD is smaller and exhibits minimal dependency on the bias voltage. In this case, the depletion region is 'frozen', thereby exhibiting limited response to bias voltage at low temperatures (Figs. 5(a) and 5(b)). At elevated temperatures, the electrons trapped in the deeper-energy level defects are able to jump across to the conduct band (Fig. 5(c)), and therefore these defects become detectable in DLTS spectra. However, the lower-level defect (E_{t1}), consistently residing above the Fermi energy level, remains undetectable. Only after annealing at a specific temperature, due to the decrease in the defects and the subsequent reduction of the compensation effect, the Fermi level would shift above the E_{t1} level (Fig. 5(d)). As a result, the lower-energy level defect (E_{t1}) can respond to the voltage applied, resulting in their reappearance in the DLTS spectra.

4. Conclusion

In conclusion, this research meticulously examined the impact of 10 MeV electron irradiation on 4H-SiC SBD devices across a broad spectrum of doses. Our findings underscore that the crystal structure of SiC remains unaffected by 10 MeV electron irradiation below 3000 kGy. Subsequently, we investigated the evolution of defects in SiC under electron irradiation with increasing doses. The PL spectra demonstrate a linear increase in defect concentration correlating with the irradiation dose. The results of $I-V$ and $C-V$ measurements reveal electron irradiation at higher doses can prompt a transformation of the doping characteristics from n-type to semi-insulating. However, annealing at a relatively low temperature of 800 K can induce a notable reduction in resistance, which is owing to the elimination of unstable defects such as silicon vacancies.

Furthermore, the DLTS results revealed the prevalence of carbon vacancy defects in both pre-annealed and post-annealed 4H-SiC samples. This finding implies that SiC, when grown with a higher C : Si ratio, may exhibit increased resistance to irradiation. In addition, our DLTS analysis identified a total of eleven defects in electron-irradiated SiC samples. Among eleven defects, we discovered a previously unreported stable defect labeled as R_2 ($E_C - 0.51$ eV) in SiC after electron irradiation at a dose of 1000 kGy. We attribute this R_2 defect to $(C_2)_{Si}$, considering its energy level position corresponds with the (0 $-$) transition of $(C_2)_{Si}$. Lastly, we performed a visualization of the compensation effect based on an established theoretical model.

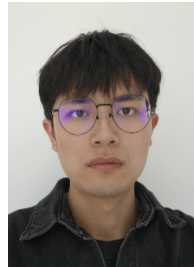
Acknowledgement

The work is supported by the Open Fund (2022E10015) of the Key Laboratory of Power Semiconductor Materials and Devices of Zhejiang Province & Institute of Advanced Semiconductors, ZJU-Hangzhou Global Scientific and Technological Innovation Center.

References

- [1] Chen X F, Yang X L, Xie X J, et al. Research progress of large size SiC single crystal materials and devices. *Light Sci Appl*, 2023, 12, 28
- [2] Lohrmann A, Iwamoto N, Bodrog Z, et al. Single-photon emitting diode in silicon carbide. *Nat Commun*, 2015, 6, 7783
- [3] Liu L Y, Liu A, Bai S, et al. Radiation resistance of silicon carbide schottky diode detectors in D-T fusion neutron detection. *Sci Rep*, 2017, 7, 13376
- [4] Lebedev A A, Kozlovski V V, Davydovskaya K S, et al. Radiation hardness of silicon carbide upon high-temperature electron and proton irradiation. *Materials*, 2021, 14, 4976
- [5] Khani M, Griepentrog G, Sokolov A, et al. Radiation hardness of Si- and SiC-power-MOSFETs in particle accelerator environments. *PCIM Eur 2022; Int Exhib Conf Power Electron Intell Motion Renew Energy Energy Manag*, 2022, 1
- [6] Emtsev V V, Ivanov A M, Kozlovski V V, et al. Similarities and distinctions of defect production by fast electron and proton irradiation: Moderately doped silicon and silicon carbide of n-type. *Semiconductors*, 2012, 46, 456
- [7] Lin Z, Yimen Z, Yuming Z, et al. Neutron radiation effect on 4H-SiC MESFETs and SBDs. *J Semicond*, 2010, 31, 114006
- [8] Dong P, Qin Y Z, Yu X G, et al. Electron radiation effects on the 4H-SiC PiN diodes characteristics: An insight from point defects to electrical degradation. *IEEE Access*, 2019, 7, 170385
- [9] Vobecký J, Hazdra P, Popelka S, et al. Impact of electron irradiation on the on-state characteristics of a 4H-SiC JBS diode. *IEEE Trans Electron Devices*, 2015, 62, 1964
- [10] Paradzah A T, Omotoso E, Legodi M J, et al. Electrical characterization of high energy electron irradiated Ni/4H-SiC Schottky barrier diodes. *J Electron Mater*, 2016, 45, 4177
- [11] Capan I, Brodar T, Pastuovič Ž, et al. Double negatively charged carbon vacancy at the h- and k-sites in 4H-SiC: Combined Laplace-DLTS and DFT study. *J Appl Phys*, 2018, 123, 161597
- [12] Son N T, Trinh X T, Løvlie L S, et al. Negative-U system of carbon vacancy in 4H-SiC. *Phys Rev Lett*, 2012, 109, 187603
- [13] Kimoto T, Niwa H, Okuda T, et al. Carrier lifetime and breakdown phenomena in SiC power device material. *J Phys D Appl Phys*, 2018, 51, 363001
- [14] Storasta L, Tsuchida H. Reduction of traps and improvement of carrier lifetime in 4H-SiC epilayers by ion implantation. *Appl Phys Lett*, 2007, 90, 062116
- [15] Nagy R, Niethammer M, Widmann M, et al. High-fidelity spin and optical control of single silicon-vacancy centres in silicon carbide. *Nat Commun*, 2019, 10, 1954
- [16] Wolfowicz G, Anderson C P, Yeats A L, et al. Optical charge state control of spin defects in 4H-SiC. *Nat Commun*, 2017, 8, 1876
- [17] Tarasenko S A, Poshakinskiy A V, Simin D, et al. Spin and optical properties of silicon vacancies in silicon carbide—A review. *Phys Status Solidi B*, 2018, 255, 1700258
- [18] Magnusson B, Son N T, Csóré A, et al. Excitation properties of the divacancy in 4H-SiC. *Phys Rev B*, 2018, 98, 195202
- [19] Son N T, Shafizadeh D, Ohshima T, et al. Modified divacancies in 4H-SiC. *J Appl Phys*, 2022, 132, 025703
- [20] Seo H, Falk A L, Klimov P V, et al. Quantum decoherence dynamics of divacancy spins in silicon carbide. *Nat Commun*, 2016, 7, 12935
- [21] Son N T, Stenberg P, Jokubavicius V, et al. Energy levels and charge state control of the carbon antisite-vacancy defect in 4H-SiC. *Appl Phys Lett*, 2019, 114, 212105
- [22] Polking M J, Dibos A M, de Leon N P, et al. Improving defect-based quantum emitters in silicon carbide via inorganic passivation. *Adv Mater*, 2018, 30, 1704543
- [23] Coutinho J. Theory of the thermal stability of silicon vacancies and interstitials in 4H-SiC. *Crystals*, 2021, 11, 167
- [24] Karsthof R, Bathen M E, Galekas A, et al. Conversion pathways of primary defects by annealing in proton-irradiated n-type 4H-SiC. *arXiv: 2007.03985*, 2020
- [25] Son N T, Carlsson P, ul Hassan J, et al. Divacancy in 4H-SiC. *Phys*

- Rev Lett, 2006, 96, 055501**
- [26] Kuate D R, Zhang X Y, Bracher D O, et al. Energetics and kinetics of vacancy defects in 4H-SiC. *Phys Rev B*, 2018, 98, 104103
- [27] Nakane H, Kato M, Ohkouchi Y, et al. Deep levels related to the carbon antisite–vacancy pair in 4H-SiC. *J Appl Phys*, 2021, 130, 065703
- [28] Kaneko H, Kimoto T. Formation of a semi-insulating layer in n-type 4H-SiC by electron irradiation. *Appl Phys Lett*, 2011, 98(26), 262106
- [29] Lebedev A A, Kozlovski V V, Davydovskaya K S, et al. Features of the carrier concentration determination during irradiation of wide-gap semiconductors: The case study of silicon carbide. *Materials*, 2022, 15, 8637
- [30] Ahoujia M, Crocket H C, Scott M B, et al. Photoluminescence characterization of defects introduced in 4H-SiC during high energy proton irradiation and their annealing behavior. *MRS Online Proc Libr*, 2004, 815, 147
- [31] Castelletto S, Johnson B C, Ivády V, et al. A silicon carbide room-temperature single-photon source. *Nat Mater*, 2014, 13, 151
- [32] Steeds J. Photoluminescence study of the carbon antisite–vacancy pair in 4H- and 6H-SiC. *Phys Rev B Condens Matter*, 2009, 80, 245202
- [33] Dietz J R, Hu E L. Optical and strain stabilization of point defects in silicon carbide. *Appl Phys Lett*, 2022, 120, 184001
- [34] Rühl M, Ott C, Götzinger S, et al. Controlled generation of intrinsic near-infrared color centers in 4H-SiC via proton irradiation and annealing. *Appl Phys Lett*, 2018, 113, 122102
- [35] Lebedev A A, Ber B Y, Seredova N V, et al. Radiation-stimulated photoluminescence in electron irradiated 4H-SiC. *J Phys D Appl Phys*, 2015, 48, 485106
- [36] Lebedev A A. Deep level centers in silicon carbide: A review. *Semiconductors*, 1999, 33, 107
- [37] Antonio C, Anna C, Lorenzo R, et al. Low temperature annealing of electron irradiation induced defects in 4H-SiC. *Appl Phys Lett*, 2004, 85, 3780
- [38] Hazdra P, Vobecký J. Radiation defects created in n-type 4H-SiC by electron irradiation in the energy range of 1–10 MeV. *Phys Status Solidi A*, 2019, 216, 1900312
- [39] Alfieri G, Monakhov E V, Svensson B G, et al. Annealing behavior between room temperature and 2000 °C of deep level defects in electron-irradiated n-type 4H silicon carbide. *J Appl Phys*, 2005, 98, 043518
- [40] David M L, Alfieri G, Monakhov E M, et al. Electrically active defects in irradiated 4H-SiC. *J Appl Phys*, 2004, 95, 4728
- [41] Alfieri G, Monakhov E V, Svensson B G, et al. Defect energy levels in hydrogen-implanted and electron-irradiated n-type 4H silicon carbide. *J Appl Phys*, 2005, 98, 113524
- [42] Hemmingsson C, Son N T, Kordina O, et al. Deep level defects in electron-irradiated 4H-SiC epitaxial layers. *J Appl Phys*, 1997, 81, 6155
- [43] Hazdra P, Záhlava V, Vobecký J, et al. Radiation defects produced in 4H-SiC epilayers by proton and alpha-particle irradiation. *Materials Science Forum*, 2013, 2266, 661
- [44] Iwata H P, Lindefelt U, Öberg S, et al. Effective masses of two-dimensional electron gases around cubic inclusions in hexagonal silicon carbide. *Phys Rev B*, 2003, 68, 245309
- [45] Szász K, Ivády V, Abrikosov I A, et al. Spin and photophysics of carbon-antisite vacancy defect in 4H silicon carbide: A potential quantum bit. *Phys Rev B*, 2015, 91, 121201
- [46] Umeda T, Son N T, Isoya J, et al. Identification of the carbon antisite–vacancy pair in 4H-SiC. *Phys Rev Lett*, 2006, 96, 145501
- [47] Karsthof R, Bathen M E, Kuznetsov A, et al. Formation of carbon interstitial-related defect levels by thermal injection of carbon into n-type 4H-SiC. *J Appl Phys*, 2022, 131, 035702



Huifan Xiong is currently working toward the PhD degree at the School of Materials Science and Engineering, Zhejiang University. His current research interests mainly include irradiation and detectors of SiC.



Lihui Song received his PhD degree at the University of New South Wales in 2015. He then worked in Hangzhou Dianzi University as an associate professor. He now works at Zhejiang University Hangzhou Global Scientific and Technological Innovation Center as a researcher. His research focuses on the impurity and defect engineering in semiconductors.



Deren Yang is an academician of the Chinese Academy of Science, president of NingboTech University, director of the Faculty of Engineering at Zhejiang University and chief scientist of Zhejiang University Hangzhou Global Scientific and Technological Innovation Center. He received his PhD in 1991, at Zhejiang University. In the 1990s, he worked in Japan, Germany, and Sweden for several years as a visiting researcher. He has been engaged in research on silicon materials for microelectronic devices, solar cells, and nanodevices.



Xiaodong Pi received his PhD degree at the University of Bath in 2004. He then carried out research at McMaster University and the University of Minnesota at Twin Cities. He joined Zhejiang University as an associate professor in 2008. He is now a professor in the State Key Laboratory of Silicon and Advanced Semiconductor Materials, the School of Materials Science and Engineering and Zhejiang University-Hangzhou Global Scientific and Technological Innovation Center. His research mainly concerns group IV semiconductor materials and devices.